Generating new magnetic properties in organic-inorganic hybrids

Wu, Jiquan; Akhtar, N.; Gengler, R. Y. N.; Palstra, T. T. M.; Rudolf, P.

IMPORTANT NOTE: You are advised to consult the publisher's version (publisher's PDF) if you wish to cite from it. Please check the document version below.

Document Version
Publisher's PDF, also known as Version of record

[Link to publication in University of Groningen/UMCG research database](#)

PAPER

Generating new magnetic properties in organic–inorganic hybrids†

J. Wu, N. Akhtar, R. Y. N. Gengler, T. T. M. Palstra and P. Rudolf*

Organic–inorganic hybrids are a rapidly developing class of multifunctional materials, which can present properties different from those of either of their building blocks. Control over the structure during the assembly process is crucial to achieve the desired functions. Here we present the layer-by-layer deposition in ambient conditions of $CoCl_4$-octahedra or $MnCl_4$-octahedra and organic layers to tailor their magnetic properties. The Langmuir–Blodgett technique used to assemble these structures provides intrinsic control over the film structure down to the molecular level. Magnetic characterization reveals that $MnCl_4$-based hybrid Langmuir–Blodgett films order antiferromagnetically like the bulk hybrid, while the $CoCl_4$-based hybrid Langmuir–Blodgett films show ferromagnetic coupling in contrast to the bulk hybrid, which is a paramagnet.

Introduction

Organic–inorganic hybrid materials have attracted significant attention due to their versatility for combining desirable properties of individual components into one single composite[1–6] but also because new properties that are absent in either of their building blocks can be generated.[2] For organic–inorganic hybrids suitable for electric and magnetic devices[7,8] an extra challenge is that thin films are the most desirable form for the active material. Langmuir–Blodgett (LB) deposition is a versatile method for thin film growth because it proceeds at room temperature and can be applied to flexible substrates; moreover it offers the possibility to exploit self-assembly and, most importantly, it provides excellent control down to molecular level through simply changing external parameters during the deposition.[9,10] This is why we have chosen this fabrication method for the work presented here, which derived inspiration from the report on paramagnetism in $CoCl_4(C_5H_6CH_2CH_2NH_3)_2$ and $MnCl_4(C_5H_6CH_2CH_2NH_3)_2$ hybrid crystals.[11] These crystals have a layered structure with polar interfaces where the interaction between the $CoCl_4^{2-}$ (or $MnCl_4^{2-}$) and NH_3^+ group has a crucial effect on the properties of the ensemble. One of the goals addressed here was to produce $CoCl_4^{2-}$ and $MnCl_4^{2-}$ based hybrids in the form of thin films with adjustable composition and thickness by using the LB method, which takes advantage of the soluble nature of precursors ($CoCl_2$, $MnCl_2$, $CuCl_2$). $CuCl_2$-based hybrid LB films have been successfully fabricated and showed ferromagnetism.[7] Similarly in the hybrid LB films reported

here, organic and inorganic parts are connected *via* hydrogen bonds between the NH_3 group and the chlorine ions from $CoCl_4^{2-}$ or $MnCl_4^{2-}$.

Differently from the bulk synthesis for $CoCl_4$- and $MnCl_4$-based hybrids, the LB technique allows not only for the modification of the interlayer spacing in the film by using different organic spacers, it permits to tune the spacing within the layer by changing the target pressure during the deposition. In the case of the $CoCl_4$-based bulk hybrid, the spacing between the coordinated Co-ions is not close enough to induce magnetic interaction.[11] Since a Co^{2+} ion has a d^7 configuration, it can be stable both with octahedral as well as with tetrahedral coordination[11] and the energy difference between these two coordinations is small. Hence we expect, by using the Langmuir–Blodgett technique, to be able to overcome the small energy difference if we apply a high enough target pressure during deposition. The goal of this work is therefore to verify whether it is possible to form corner shared $CoCl_4$ and $MnCl_4$ octahedra, thus generating new magnetic properties in the hybrid LB films.

Experiment section

Preparation of $CoCl_4$- and $MnCl_4$-based hybrid LB films

Octadecyl amine (>99%) was purchased from Alfa Aesar, cobalt chloride ($CoCl_2$; 99.999%), manganese chloride ($MnCl_2$; 99.999%), methyl ammonium chloride (MA), and other chemical reagents of analytical grade were purchased from Sigma Aldrich and used as received. To prepare octadecyl ammonium chloride ($ODAH^+Cl^-$), we used the same method as reported in ref. 7. The subphase in the LB deposition experiments was an aqueous solution of $CoCl_2/MnCl_2$ (1.0×10^{-3} mol L^{-1}) and MA (1.0×10^{-3} mol L^{-1}).

Zernike Institute for Advanced Materials, University of Groningen, Nijenborgh 4, 9747 AG Groningen, The Netherlands. E-mail: p.rudolf@rug.nl
† Electronic supplementary information (ESI) available. See DOI: 10.1039/c6tc04737h

Surface pressure–molecular area (Π–a) isotherm measurements and deposition experiments were performed using a NIMA Technology thermostated LB trough. The temperature was kept at 25 °C during these experiments. Langmuir films were obtained by spreading a chloroform–methanol (9 : 1) solution of $ODAH^+Cl^-$ (0.25 mg mL^{-1}) onto the subphase. After a 1 h waiting time to allow for solvent evaporation, the molecules were compressed at a rate of 20 cm^2 min^{-1} by a movable barrier until a desired surface pressure was reached and this pressure was kept constant throughout the whole deposition process. The compressed Langmuir film was allowed to stabilize for 30 minutes time before deposition. LB films were deposited by vertical dipping of hydrophobic substrates (see below) into the subphase at a dipping speed of 5 mm min^{-1}.

X-ray photoelectron spectroscopy (XPS)

150 nm thick films of gold (purity 99.99%, Schöne Edelmetaal B.V.), grown on glass microscope slides (Knittel glass) served as substrates for the XPS measurements of the $CoCl_4$-based hybrid LB film. Silicon wafers (Prime Wafer) served as substrates for XPS measurements of the $MnCl_4$-based hybrid LB film. Both the substrates were made hydrophobic by modifying surface with octadecyltrichlorosilane prior to the LB film deposition.[12] XPS data were collected using a Surface Science SSX-100 ESCA instrument with a monochromatic Al K$_\alpha$ X-ray source ($h\nu$ = 1486.6 eV) operating at a base pressure of $\approx 5 \times 10^{-10}$ mbar. XPS spectra were analysed using the least-squares curve fitting programme Winspec developed at the LISE laboratory, University of Namur, Belgium. The energy resolution was set to 1.26 eV. Binding energies (BEs) are reported with a precision of ± 0.1 eV, and referenced to the C 1s (BE = 285.6 eV) photoemission peak.[13] All measurements were carried out on freshly prepared samples; four different spots were measured on each sample to check for reproducibility.

X-ray diffraction (XRD)

Diffraction measurements were performed on 18-layer-thick $CoCl_4$-based and 20-layer-thick $MnCl_4$-based hybrid LB films, which were deposited on glass microscope slides (Knittel glass) made hydrophobic as described above for Au films and silicon wafers. The out-of-plane X-ray reflectivity data for the hybrid films were collected under ambient conditions with a Philips PANanalytical X'Pert MRD diffractometer, equipped with a Cu K$_\alpha$ (λ = 1.5418 Å) radiation source (operated at 40 keV, 40 meV); a 0.25° divergence slit and a 0.125° antiscattering slit were employed. The 2θ scans from 0.6° to 15° were collected with a 0.02° step and a counting time of 15 s per step.

Magnetic characterization of the $CoCl_4$/$MnCl_4$-based hybrid LB films

The magnetic properties were measured using a Quantum Design XL SQUID Magnetometer. The samples, a 1724-layer-thick $CoCl_4$-based and a 1884-layer-thick $MnCl_4$-based hybrid LB film on glass substrates (Knittel Glass, 0.1 mm thick, made hydrophobic as described above), were mounted in a gelatin capsule, which was fixed in a plastic straw.

Results and discussion

Assembly of $CoCl_4$ and $MnCl_4$-based hybrid Langmuir films and transfer to the substrate

To optimize the quality of the films deposited by the Langmuir–Blodgett technique, we studied the properties of the hybrid Langmuir film assembled at the air–water interface. Fig. 1 displays the surface pressure–area per molecule (Π–a) isotherms of $ODAH^+Cl^-$ on the $CoCl_2$–MA (a) and $MnCl_2$–MA (b) subphases. Both of the Π–a isotherms show typical and clear phase transitions during the compression process. In order to get densely packed monolayers, we chose target pressures of 38 mN m^{-1} and 47 mN m^{-1} for the $CoCl_2$ and $MnCl_2$ hybrids respectively; these target pressures are far away from the pressures where the 2D solid layers collapse (52 mN m^{-1} for the $CoCl_2$ hybrids and 56 mN m^{-1} for the $MnCl_2$ hybrids).

Proof for successful transfer of the Langmuir films comes from the transfer characteristics plotted in Fig. 1(c) and (d). The blue line in the lower panel of Fig. 1 shows the displacement of the substrate as a function of time, which corresponds to dipping into the subphase; the black curve represents the trough area covered by the $ODAH^+$–$CoCl_4$ or $ODAH^+$–$MnCl_4$, recorded as a function of deposition time. When the substrate moves into the subphase during each dip, the trough area reduces due to the transfer of part of the Langmuir film from the subphase surface to the substrate. The transfer ratio is 1 if the decrease in area is equal to the substrate surface area. In the present case, the transfer ratio was unity for the downward stroke and 0.97 $\pm$ 0.04 for the upward stroke for both films, suggesting Y-type deposition.[14]

Mechanism of $CoCl_4$/$MnCl_4$-based hybrid LB film deposition

The proposed structure of the $CoCl_4$/$MnCl_4$-based hybrid LB film is sketched in Fig. 2; the $CoCl_4^{2-}$ or $MnCl_4^{2-}$ layer is composed of 6 octahedral Cl$^-$ encaging the central Co^{2+} or Mn^{2+} ions, four of which share neighbouring Cl$^-$ in plane, one from the amphiphilic $ODAH^+Cl^-$ and another one from the MA in the subphase. Such a corner-shared octahedral structure has been reported for $CuCl_4$-based hybrid LB film,[7] for which the self-assembly mechanism is almost the same as for the $CoCl_4$/$MnCl_4$-based hybrid LB films we report on here.

In contrast to this film structure, the $CoCl_4(C_5H_6CH_2CH_2NH_3)_2$ bulk hybrid consists of free-standing tetrahedral $CoCl_4^{2-}$ in an organic $C_5H_6CH_2CH_2NH_3$ matrix held together by the hydrogen-bond network.[11] $MnCl_4(C_5H_6CH_2CH_2NH_3)_2$ bulk hybrids have a symmetric coordination of $C_5H_6CH_2CH_2NH_3$ ligands on both sides of the octahedral corner-shared $MnCl_4^{2-}$ sheets.[11]

Composition of the $CoCl_4$/$MnCl_4$-based inorganic sheets

To verify the composition of the films, X-ray photoelectron spectroscopy (XPS) data were collected from 17-layer-thick $CoCl_4$/$MnCl_4$-based hybrid LB films as well as $CoCl_4(C_6H_5CH_2CH_2NH_3)_2$ and $MnCl_4(C_6H_5CH_2CH_2NH_3)_2$ bulk hybrids; all four samples are layered materials in which the charged MCl_4^{2-} (M = Co or Mn) are bonded with an amine group at the organic–inorganic interface.
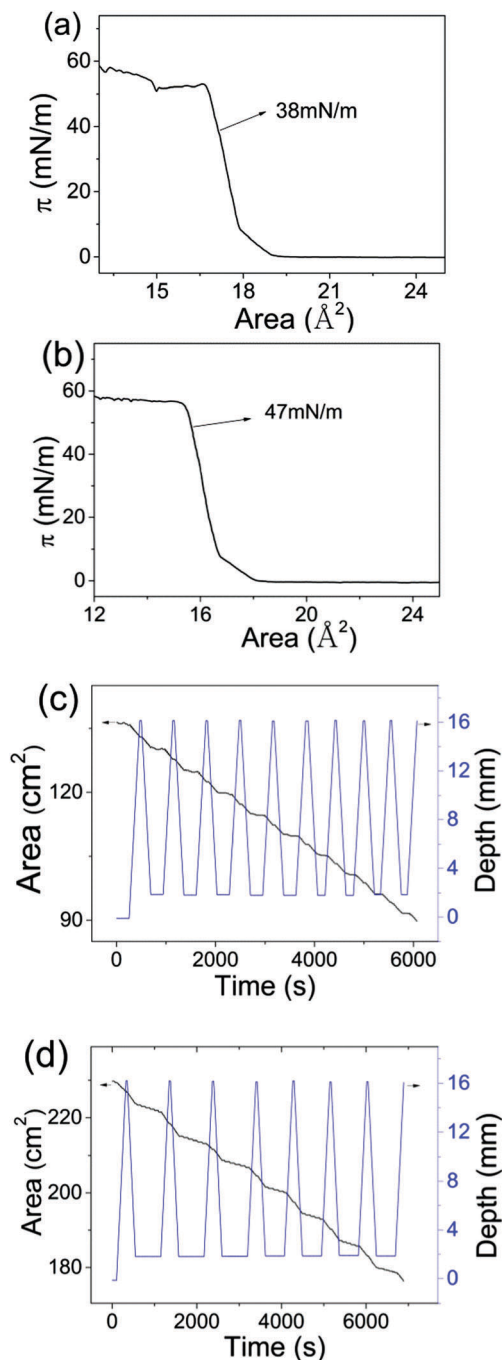
This journal is © The Royal Society of Chemistry 2017

J. Mater. Chem. C, 2017, 5, 1782–1788 | 1783

Fig. 1 $\Pi-a$ isotherms of ODAH$^+$Cl$^-$ on an aqueous CoCl$_2$–MA (a) and MnCl$_2$–MA (b) subphase. Lower panel: Deposition of a CoCl$_4$-based hybrid LB film (c) and a MnCl$_4$-based hybrid LB film (d).

The photoemission spectra of the Co $2p_{3/2}$ core level regions of the bulk compound and the hybrid film are shown in Fig. 3(a) and (b), respectively, while the corresponding Mn $2p_{3/2}$ core level regions are plotted in Fig. 4(a) and (b). All four spectra show a shake-up satellite at the high binding energy side of the main peak, which is a signature of Co/Mn being in the 2+ oxidation state.[15,16]

The Co $2p_{3/2}$ spectrum for the bulk hybrid can be fitted with a single component peaked at a binding energy of 781.9 eV
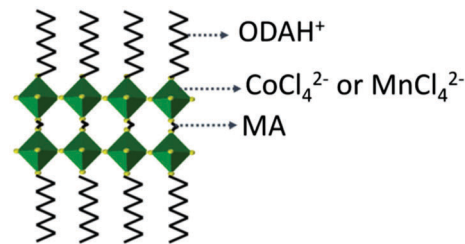

Fig. 2 Scheme of the proposed structure of the CoCl$_4$/MnCl$_4$-based hybrid LB films.

which corresponds to Co–Cl bonds within the tetrahedra;[17] the shake-up satellite was fitted with three peaks at binding energies of 783.8 eV, 787.2 eV and 789.7 eV. The BEs of the Co $2p_{3/2}$ line for the LB film (782.5 eV) and of the shake-up satellite peaks (784.9 eV, 787.4 eV, and 791.0 eV) are higher than those of the bulk hybrid. Since it has been reported that the binding energy of core level electrons for Co^{2+} in octahedral coordination is larger than for those in tetrahedral coordination,[18] this is an indication that in the hybrid LB films, the Co–Cl bonds are part of the octahedral corner-shared CoCl$_4$-based inorganic sheets.

A detailed scan of the Cl $2p$ core level region for the CoCl$_4$(C$_6$H$_5$CH$_2$CH$_2$NH$_3$)$_2$ bulk hybrid and the CoCl$_4$-based hybrid LB films are shown in Fig. 3(c) and (d), respectively. The spectrum of the bulk hybrid is peaked at a binding energy of 199.6 eV, which identifies it as due to Cl–Co bonds in tetrahedra in agreement with the X-ray diffraction measurements by A. H. Arkenbout;[11] the lower BE for the hybrid LB films (198.9 eV), points to Cl–Co bonds in octahedra.

The spectrum of the Mn $2p_{3/2}$ line for the bulk hybrid (Fig. 4(a)) can be fitted with one single main peak at BE = 642.1 eV, which can be assigned to Mn–Cl bonds within the octahedra; the shake-up satellite peak at BE = 647.6 eV confirms the 2+ state of Manganese. The Mn $2p_{3/2}$ line for MnCl$_4$-based hybrid LB films can be fitted with a main peak and a satellite at the same binding energies, indicating that we have Mn^{2+} in octahedral coordination with Cl$^-$ also in this case. However, the Mn $2p_{3/2}$ spectra of both the MnCl$_4$-based hybrid LB films and the bulk hybrid require in the fit an additional component at BE = 643.5 eV; the latter originates from oxidized manganese,[19] the presence of which is supported by a much stronger oxygen peak in the survey spectrum shown in Fig. 5 as compared to the CoCl$_4$-based hybrid film.

The scan of the Cl $2p$ core level region for both the bulk hybrid of MnCl$_4$(C$_6$H$_5$CH$_2$CH$_2$NH$_3$)$_2$ and the MnCl$_4$-based hybrid LB film are shown in Fig. 4(c) and (d); the spectra are both peaked at BE = 198.6 eV, corresponding to Cl–Mn bonds in the octahedra.[11]

Additionally, in order to further confirm the octahedral coordination of Co^{2+} in the CoCl$_4$-based hybrid film, the UV/visible absorption spectra were measured (shown in the ESI†). Since the energy separation between the e_g and t_{2g} orbitals in the octahedral field is larger than in the tetrahedral one, the absorption bands of Co^{2+} in tetrahedral symmetry are found at wavelength
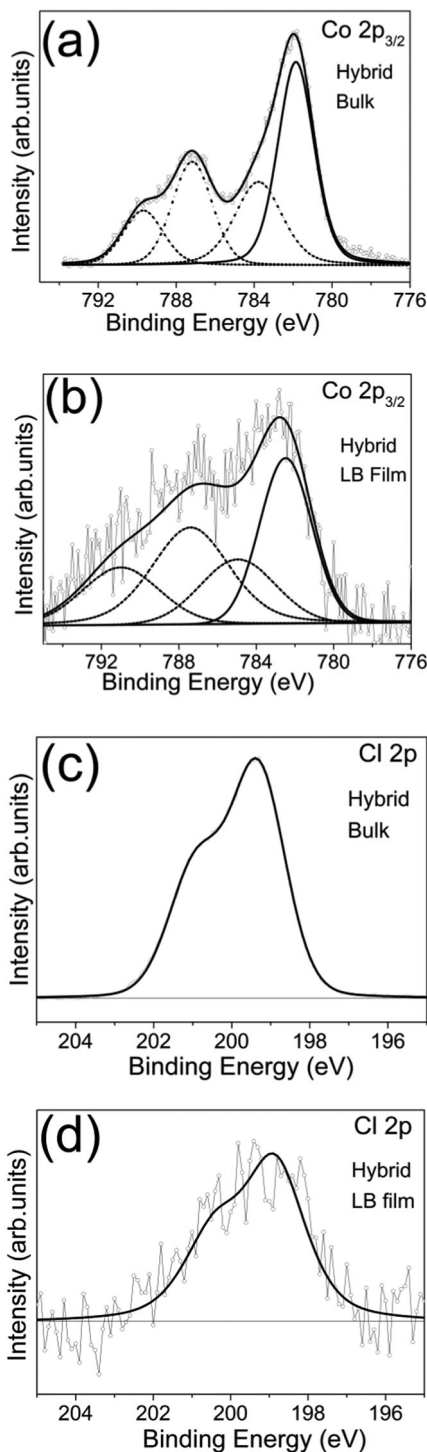
Fig. 3   X-ray photoemission spectra of the Co $2p_{3/2}$ and Cl 2p core level regions of a CoCl$_4$-based bulk hybrid (top panels) in powder form and of a 17-layer-thick CoCl$_4$-based hybrid LB film (bottom panels); fits to the experimental lines are also shown.
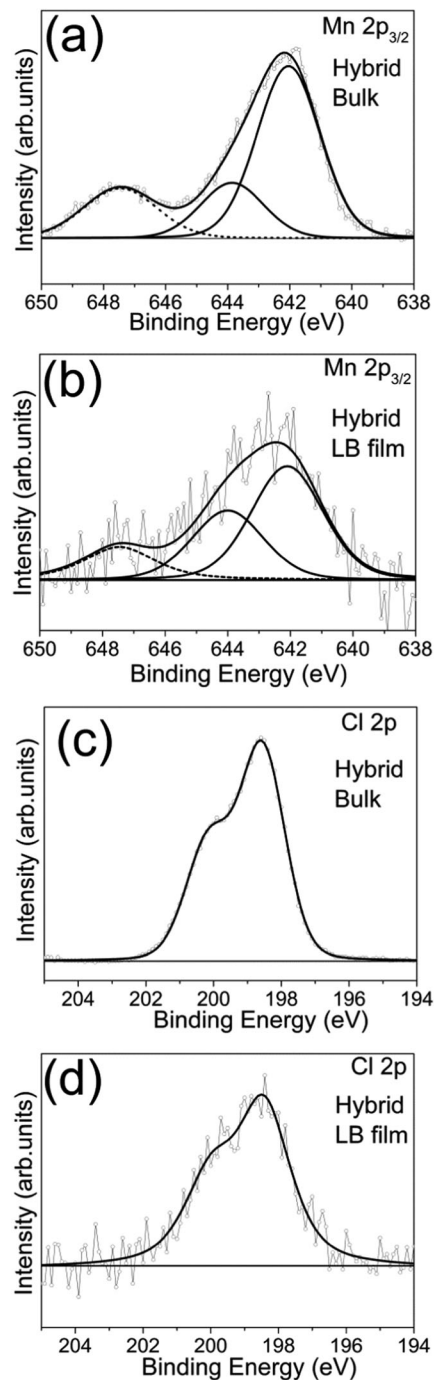

Fig. 4   X-ray photoemission spectra of the Cl 2p, Mn $2p_{3/2}$ core level regions of a 17-layer-thick hybrid LB film (right panels) and a MnCl$_4$-based bulk hybrid (left panels) in powder form and fits to the experimental lines.

of 524 nm, 610 nm and 660 nm,[20] while Co^{2+} in octahedral symmetry absorbs at shorter wavelengths.[21] The absorption band at the wavelength of 476 nm observed for CoCl$_4$-based hybrid LB films therefore clearly points to Co^{2+} in an octahedral environment.

Structure of the CoCl$_4$/MnCl$_4$-based hybrid film

To gain insight into the structure of the films and to prove the high quality of the layer-by-layer deposition, X-ray diffraction studies were carried out. Fig. 6 shows the specular X-ray reflectivity of an 18-layer-thick of CoCl$_4$-based and a 20-layer-thick MnCl$_4$-based hybrid LB film, deposited at Π = 38 mN m^{-1} and 47 mN m^{-1}, respectively. Diffraction peaks as well as Kiessig fringes are observed for both films and provide evidence for a
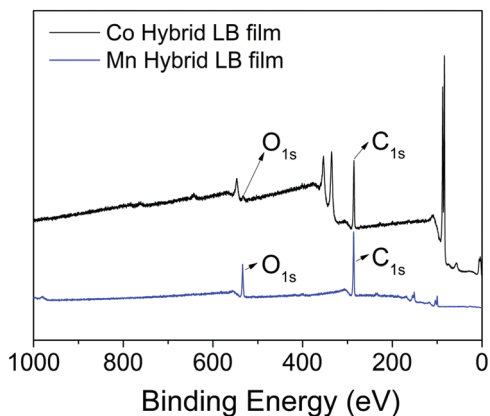
Fig. 5   X-ray photoemission survey spectra (XPS) of CoCl$_4$- and MnCl$_4$-based hybrid LB films.

well-ordered layered structure; the Kiessig fringes in particular indicate that the LB films remain relatively smooth during multilayer deposition.

The length of the smallest periodic unit perpendicular to the film surface, d, calculated from the positions of the diffraction peaks for CoCl$_2$/MnCl$_2$-based hybrid LB films by using the Bragg formula was found to be 52.1 $\pm$ 0.5 Å/52.5 $\pm$ 0.5 Å. It should be noted that based on geometrical considerations, the expected d value is $\approx$59 Å, which is larger than the observed experimental value. Since the long ODAH$^+$Cl$^-$ molecules have a tendency to adopt a tilted conformation, the lower d value observed most likely arises from the tilting of these molecules with respect to the film plane. The tilt angle of CoCl$_2$/MnCl$_2$-based hybrid LB films would then be $\approx$28°/$\approx$27° as sketched on the left hand side in Fig. 6(c) and (d).

Kiessig fringes result from the interference of X-rays reflected from the surface of the film and from the film/substrate interface as a consequence of the angle-dependent phase shift. Their period is determined by the thickness of the film.[22] A layered material with n repeat units shows n-2 Kiessig fringes between two diffraction peaks in the X-ray reflectivity spectrum.[23]

Based on the modified Bragg law,[22,24] the total thickness of 447 Å and 499 Å can be extracted CoCl$_4$-based and MnCl$_4$-based hybrid LB films respectively, which is close to what we expect from the d-spacing result, namely 475 Å and 524 Å.

Magnetic order

Magnetism in organic–inorganic hybrids arises from the transition metal ions in the inorganic sheets. Magnetization measurements were performed on a 1724-layer-thick CoCl$_4$-based and a 1884-layer-thick MnCl4-based hybrid LB film. The large film thickness was necessary in order to obtain a measurable magnetic moment.

The magnetization loop measured at 3 K with the field applied both in and out of the plane of the CoCl$_4$-based hybrid LB film shows magnetic order resulting in the ferromagnetic hysteresis loop (Fig. 7(a)) differently from the CoCl$_4$(C$_6$H$_5$CH$_2$CH$_2$NH$_3$)$_2$ bulk hybrid, which shows no magnetic order down to 2 K.[11] The coercive
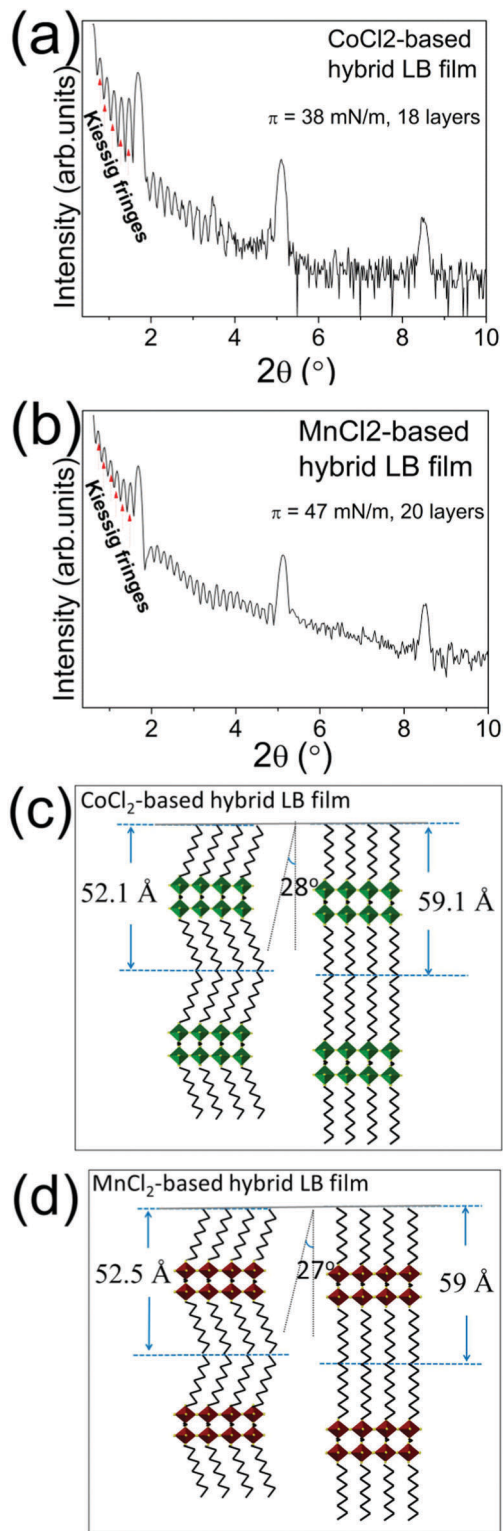

Fig. 6   X-ray specular reflectivity patterns of (a) a CoCl$_4$-based hybrid LB film (with an ordered structure as sketched in (c)) and (b) a MnCl$_4$-based hybrid LB film (with an ordered structure as sketched in (d)).

field of both the in and out of plane configuration is 200 Oe at 3 K. These results indicate that the high surface pressure applied during deposition was sufficient to induce the Co-ions to pack
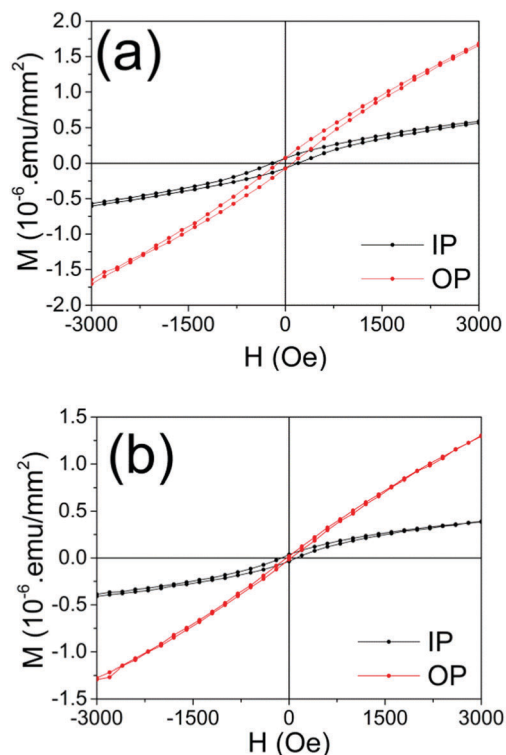
Fig. 7 Magnetization *versus* field at 3 K measured both in plane (IP) and out of plane (OP) for (a) a 1724-layer-thick $CoCl_4$-based hybrid LB film; (b) a 1884-layer-thick $MnCl_4$-based hybrid LB film.

closely enough to induce magnetic exchange interaction. Comparing to the bulk hybrid $CoCl_4(C_6H_5CH_2CH_2NH_3)_2$, the situation is different in the $CoCl_4$-based hybrid LB film, where, because of the octahedral coordination, the Co^{2+} ($S = 3/2$) are Jahn–Teller active and involved in coherent orbital ordering, which causes magnetic coupling in the plane of the inorganic sheets.[25,26] Considering that the $M–H$ loop shows the same S-shape without saturating at higher magnetic field it is equally possible that this ferromagnetic moment is caused by the canting of antiferromagnetically coupled moments. This hypothesis is supported by the negative Weiss temperature, calculated from the $1/M–T$ data (shown in the ESI†).

The magnetization loop measured at 3 K with the field applied both in and out of the plane for the $MnCl_4$-based hybrid LB film shows a small hysteresis (Fig. 7(b)) with a coercive field of around 120 Oe in the in-plane configuration and 30 Oe in the out-of-plane configuration. The Weiss temperature calculated from $1/M–T$ data is also negative, indicating antiferromagnetic exchange interaction, which is the same as in the bulk hybrid $MnCl_4(C_6H_5CH_2CH_2NH_3)_2$. The hysteresis of both the hybrid LB film and bulk hybrid is due to the ferromagnetic component in the long range ordered states, as a result of the canting of the antiferromagnetically ordered spins.[11]

Conclusion

We synthesized a new type of $CoCl_4$-based hybrid LB film with an octahedrally coordinated inorganic layered structure, which is different from tetrahedrally coordinated one in the $CoCl_4$-based bulk hybrid. The new structure of the hybrid LB film goes hand-in-hand with the generation of new magnetic properties, namely antiferromagnetic exchange resulting in ferromagnetic ordering. Most importantly, the ferromagnetic order parameter, the remanent magnetisation, can be modified by changing the number of layers. This means that for certain practical applications, this material can still be used as a ferromagnet.

A $MnCl_4$-based hybrid LB film was also successfully synthesized but in this case the structure and magnetic properties were similar to those of the corresponding bulk hybrid. These results indicate that the assembly by the LB technique allows to tailor the layer-by-layer structure easily and to induce new magnetic properties, which make these LB films promising candidates for applications in electronics.

References

1 B. Kundys, A. Lappas, M. Viret, V. Kapustianyk, V. Rudyk, S. Semak, C. Simon and I. Bakaimi, *Phys. Rev. B: Condens. Matter Mater. Phys.*, 2010, **81**, 224434.

2 A. O. Polyakov, A. H. Arkenbout, J. Baas, G. R. Blake, A. Meetsma, A. Caretta, P. H. M. van Loosdrecht and T. T. M. Palstra, *Chem. Mater.*, 2011, **24**, 133.

3 P. Jain, V. Ramachandran, R. J. Clark, H. D. Zhou, B. H. Tobey, N. S. Dalal, H. W. Kroto and A. K. Cheetham, *J. Am. Chem. Soc.*, 2009, **131**, 13625.

4 D. W. Fu, W. Zhang, H. L. Cai, Y. Zhang, J. Z. Ge, R. G. Xiong, S. D. Huang and T. Nakamura, *Angew. Chem., Int. Ed.*, 2011, **50**, 11947.

5 R. Plass, S. Pelet, J. Krueger, M. Grätzel and U. Bach, *J. Phys. Chem. B*, 2002, **106**, 7578.

6 N. Akhtar, A. O. Polyakov, A. Aqeel, P. Gordiichuk, G. R. Blake, J. Baas, H. Amenitsch, A. Herrmann, P. Rudolf and T. T. M. Palstra, *Small*, 2014, **10**, 23.

7 D. B. Mitzi, *IBM J. Res. Dev.*, 2001, **45**, 29.

8 S. A. DiBenedetto, A. Facchetti, M. A. Ratner and T. J. Marks, *Adv. Mater.*, 2009, **21**, 1407.

9 M. Clemente-León, E. Coronado, A. Soriano-Portillo, E. Colacio, J. M. Dominguez-Vera, N. Galvez, R. Madueno and M. T. Martin-Romero, *Langmuir*, 2006, **22**, 6993.

10 M. Petruska, B. Watson, M. Meisel and D. Talham, *Chem. Mater.*, 2002, **14**, 2011.

11 A. H. Arkenbout, *Organic–Inorganic Hybrids: a Route Towards Soluble Magnetic Electronics*, PhD thesis, University of Groningen, 2010.

12 G. Andreatta, Y. J. Wang, F. K. Lee, A. Polidori, P. Tong, B. Pucci and J.-J. Benattar, *Langmuir*, 2008, **24**, 6072.

13 M. Dubey, I. Gouzman, S. L. Bernasek and J. Schwartz, *Langmuir*, 2006, **22**, 4649.

14 M. C. Petty, *Langmuir-Blodgett Films*, Cambridge University Press, 1996.

15 N. S. McIntyre and M. G. Cook, *Anal. Chem.*, 1975, **47**, 2208.

16 S. R. Sarath Kumar, M. N. Hedhili, H. N. Alshareef and S. Kasiviswanathan, *Appl. Phys. Lett.*, 2010, **97**, 111909.

17 S. Suzer, F. Kadirgan and H. M. Sohmen, *Sol. Energy Mater. Sol. Cells*, 1999, **56**, 183.

18 H. G. Karge and D. Weitkamp, *Molecular Sieves 5*, Science and Technology Characterization II, 2007, p. 445.

19 W. Hummel, U. Berner, E. Curti, F. J. Pearson and T. Thoenen, *Nagra/PSI Chemical Thermodynamic Data Base*, 2002, p. 188.

20 E. M. El Malki, D. Werst, P. E. Doan and W. M. H. Sachtler, *J. Phys. Chem. B*, 2000, **104**, 5924.

21 G. Fierro, M. A. Eberhardt, M. Houalla, D. M. Hercules and W. K. Hall, *J. Phys. Chem.*, 1996, **100**, 8468.

22 J. Als-Nielsen and D. McMorrow, *Elements of Modern X Ray Physics*, John Willey & Sons Ltd, 2001.

23 U. Pietsch, V. Holy and T. Baumbach, *High-resolution X-ray scattering: From Thin Films to Lateral Nanostructures*, Springer, 2004.

24 I. Kojima and B. Li, *Rigaku J.*, 1999, **16**, 2.

25 J. H. Ammeter and J. D. Swalen, *J. Chem. Phys.*, 1972, **57**, 678.

26 J. Ferguson, D. L. Wood and K. Knox, *J. Chem. Phys.*, 1963, **39**, 881.